Pre-Clinical Research Report

Journal of INTERNATIONAL MEDICAL RESEARCH

Journal of International Medical Research
2019, Vol. 47(10) 5155–5173

DOI: 10.1177/0300060519860704
journals.sagepub.com/home/imr
SAGE

Healing physiology following delayed surgery for femoral midshaft fracture caused by high-energy injury: an *in vivo* study in dogs

Zhijun Pan[1], Jingxin Pan[2], Hanli Wang[1], Zhou Yu[3], Zhong Li[4], Wenxue Yang[2], Jing Li[1], Qingsheng Zhu[1] and Zhuojing Luo[1]

Abstract

Objective: An experimental model of severe soft tissue damage was designed to simulate high-energy fracture and observe the fracture healing process following early surgery and surgery delayed by 1 week.

Methods: Forty dogs were randomized to Group A (immediate surgery) and B (delayed surgery). The femur was broken, and the two ends were forcefully stabbed to damage the surrounding soft tissues. The fracture was repaired using a custom six-hole steel plate. Four dogs were killed on day 3 and weeks 1, 2, 4, and 8 following bone fracture. Soft tissue and bone were examined by light and electron microscopy.

Results: In Group A, no callus was present at 1, 2, 4, and 8 weeks following fracture, resulting in atrophic nonunion. In Group B, visible weak external callus was present 1 week following fracture, and good external callus growth was present at 2, 4, and 8 weeks, leading to callus healing.

Conclusion: These findings suggest that the first week is critical for fracture healing. Absence of callus in the early stage is indicative of absence of callus growth throughout the entire healing process, while the presence of callus in the early stage is indicative of vigorous callus growth thereafter.

[1]Department of Orthopedics, Xijing Hospital, Fourth Military Medical University, Xi'an, Shaanxi, China
[2]Department of Orthopedics, The Fourth Hospital of Yulin, Yulin, Shaanxi, China
[3]Department of Burn, Xijing Hospital, Fourth Military Medical University, Xi'an, Shaanxi, China
[4]Department of Orthopedics, Xi'an Honghui Hospital, Xi'an, Shaanxi, P.R. China

Corresponding authors:
Hanli Wang and Zhijun Pan, Department of Orthopedics, Xijing Hospital, Fourth Military Medical University, 127 West Changle Road, Xi'an, Shaanxi 710054, China.
Emails: 437438255@qq.com; ylpanzhijun@163.com

Keywords
Femoral midshaft fracture, high-energy injury, healing, callus, surgery, canine model

Date received: 19 September 2018; accepted: 10 June 2019

Introduction

Delayed union and nonunion are often associated with high-energy injury,[1,2] but the exact mechanisms are poorly understood. Certain studies have revealed that tibial shaft fractures accompanied by serious soft tissue damage caused by high-energy compaction often result in malunion.[3] High-energy injury damages the blood supply to the fracture ends, impairing healing[4–8]; however, early observations suggested that reoperation at the nonunion site tended to further damage the blood supply while still leading to enhanced fracture healing.[9] In addition, one study demonstrated that patients with atrophic nonunion were unlikely to develop ischemia at the fracture site and that this ischemia was required to increase osteoblast activity for promotion of fracture healing[10]; however, this is controversial.[11] Brownlow et al.[12] demonstrated that early recovery of the blood supply at the fracture site is essential for fracture healing. Their study also demonstrated that abundant revascularization in the late stage was unable to automatically trigger the fracture healing process, leading to nonunion with a rich blood supply.[12] Therefore, it may be hypothesized that the critical processes triggering fracture healing occur in the early stage of fracture.

Certain studies have indicated that post-fracture callus growth, which represents the bone healing capacity, is closely associated with damage to surrounding soft tissues[13] and that delayed union and nonunion caused by high-energy injury must be associated with even more severe soft tissue damage.[1,2,14] Severe soft tissue injury may lead to a greater local inflammatory response and poorer fracture healing. The physiological process of fracture healing is presently considered to involve benign inflammation caused by low-energy injury;[15–17] however, a model of bone fracture focusing on soft tissue damage and the inflammatory response has not been reported. Therefore, whether the healing process of a high-energy fracture is identical to that of low-energy fracture remains unclear.

In the present study, an experimental model of severe soft tissue damage was designed to simulate high-energy fracture, and the characteristics of healing of such fractures were examined. This model was used to observe the fracture healing process following early surgery and surgery delayed by 1 week.

Materials and methods

Animals

Forty normal adult Beagle dogs were provided by the Experimental Animal Center of the Fourth Military Medical University (Xi'an, China). The dogs were 6 to 12 years old, and their mean weight was 9.0 ± 1.5 kg (range, 8–12 kg). The animals were kept in single cages at a room temperature of 20°C to 26°C, humidity of 40% to 70%, 12-/12-hour light/dark cycle. They were fed 500 g of experimental dog feed each morning and had free access to drinking water. The length and diameter of their femurs were 110 to 150 mm and 12 to 15 mm, respectively. There was no difference in

sex, age, or body weight between the two experimental groups (immediate vs. delayed surgery). All animals were healthy and had no trauma or malformation at the site to be operated. This study was approved by the ethics committee of the Fourth Military Medical University (Xi'an, China). All experimental procedures were performed in accordance with the criteria for animal experiments issued by the Fourth Military Medical University (Xi'an, China) and by the National Institutes of Health.

Experimental design

High-energy injury is caused by the extremely high energy released from a raw smash, which induces extensive tissue injury. The degree of muscle damage is not easily monitored and is thus often overlooked. To highlight the effects of damage of simple muscle injury factors on the fracture healing ability, we created simple closed fractures and used the fracture ends to severely puncture the adjacent muscles to mimic the muscle injuries in a high-energy fracture. Because the pin sites of the external fixed frame are very difficult to manage, internal fixation with a Kirschner wire was used for temporary fixation in this study. The 40 dogs were randomized into Group A (immediate surgery) and Group B (delayed surgery) using a random number table ($n = 20$ per group). The dogs were anesthetized by subcutaneous injection of tiletamine/zolazepam (Zoletil 50®; Virbac, Carros, France) at a dose of 6 mg/kg. Routine hair shaving, disinfection, and draping were conducted. Needle markers were separately subcutaneously inserted from the greater trochanter and femoral condyle, and the two needles were kept in parallel but perpendicular to the longitudinal axis of the femur to determine the center of the femoral shaft. At the center of the femoral shaft, a 2.0-mm-diameter Kirschner wire was subcutaneously inserted to the bone cortex through the muscular layer and penetrated the bicortex perpendicular to the femoral shaft. The wire was retracted to the medullary cavity and inclined approximately 25° to the front and rear sides to drill two holes through the contralateral bone cortex. The wire was retracted, slid backward 2 to 3 mm along the femoral surface in the same plane to drill through the ipsilateral bone cortex, and inserted into one of the contralateral holes. At this time, five holes had been drilled in the shaft in the same plane (Figure 1) to decrease the bone strength.

A cloth pillow was placed under the inner side of the medial femoral condyle as a support, while the femoral head was used as the other support. The femur was then pressed inward from the puncture site at the center of the lateral femoral shaft to induce bending and fracture of the femur. The pin holes of the Kirschner wire on the skin then shrink naturally, with extremely minimal bleeding. The procedures were conducted under aseptic conditions, and the fracture was similar to a closed fracture.

The femoral condyle and greater trochanter were held and twisted in opposite directions through the needle markers. The two fracture ends were used to puncture the periosteum and adjacent muscles 10 times along the surface of the contralateral femoral shaft. The tissues 360° around the fracture ends were divided into five parts, with each part (72°) punctured twice, and the depth of a single puncture was 4 cm (the fracture ends were overlapped by 4 cm, and the distance between the two needle markers was reduced by 4 cm under the guidance of a graduated ruler). The total area of the puncture in the soft tissues at both ends was 8 cm, which was three-fold the diameter of the bone shaft and reached the volume of soft tissue injury in a regular high-energy fracture (magnetic resonance imaging demonstrated that the area of soft tissue injury was higher than that in

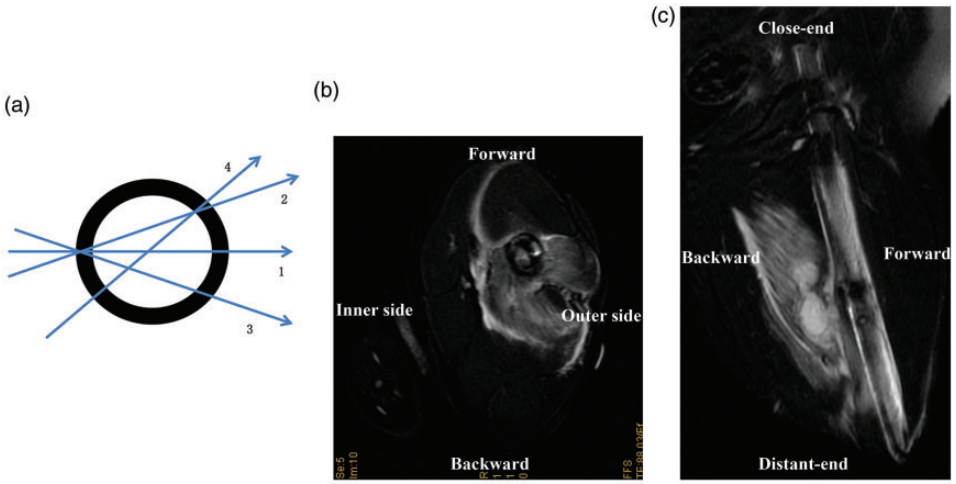

Figure 1. (a) Drill paths for drilling holes in the femur of dogs to create a site with decreased bone strength for the high-energy fracture model. (b) Fine titanium Kirschner wire was used for temporary fixation of the fracture at 4 h after fracture. Axial T2-weighted magnetic resonance imaging showed that the transverse puncture of the soft tissues was almost two-fold the femoral diameter. (c) Sagittal T2-weighted magnetic resonance imaging showed that the area of the longitudinal puncture of the soft tissues was six-fold the femoral diameter.

Tscherne grade II closed soft tissue injuries, shown in Figure 1(b) and (c)). No external signs of soft tissue injuries were found. Therefore, 40 dog models of concealed high-energy fracture were successfully established.

Surgical treatment

Dogs in Group A immediately underwent open reduction with internal fixation using custom-made six-hole stainless steel plates with a length of 60 mm (2/5 the average length of bones), width of 8 mm (1/4 the bone circumference), and thickness of 3 mm. Dogs in Group B underwent manual reduction and subcutaneous insertion of a 2.0-mm-diameter Kirschner wire into the medullary cavity via the greater trochanter to temporarily fix the fracture ends, thereby preventing the fracture ends from further stabbing the surrounding tissues. The animals were placed in their cages and the Kirschner wire was removed under sterile conditions after 7 days, followed by open reduction with internal fixation using the custom-made six-hole steel plates. The dogs' respiratory rate and heart rate were monitored using a stethoscope once every half hour until the dogs were completely conscious and could walk freely. All surgeries were performed by the same group of surgeons. Following surgery, the animals received no antibiotics or anti-inflammatory drugs, and they were well-fed and free to perform activities. All animals in each group woke from anesthesia at 3 to 5 hours following surgery, gradually began moving freely, and had resumed normal eating by 16 hours. No dogs developed infection. The animals were killed by intravenous injection of 500 mg of thiopental sodium (Shanghai New Asia Pharmaceutical Co., Ltd., Shanghai, China). Awareness and pain were monitored after the injection.

Following loss of consciousness, 20 mL of 10% potassium chloride was intravenously injected, after which the dogs' respiration and heartbeat immediately stopped.

Postoperative observation

Postoperative observation mainly included monitoring of diet, activity, and other systemic conditions; local wound healing and swelling of the affected limb; and the callus status following sampling.

Histological examination

Four dogs in each group were killed on day 3 and at weeks 1, 2, 4, and 8 following bone fracture. Tissue specimens from the fracture site were obtained to grossly observe the growth of the fracture end and its surrounding tissues, followed by hematoxylin and eosin staining (room temperature for 40 minutes) of paraffin sections (10% formalin fixation at room temperature for >24 hours; slice thickness, 5 μm) and van Gieson's staining (room temperature for 30 minutes) of plastic sections to observe the callus status. The chemotaxis of the inflammatory cells in the early stage and growth of the callus in the later stage were observed. The sections (hematoxylin and eosin staining) of the specimens on day 3 after fracture were obtained and observed under a high-magnification microscope to count the number of neutrophils in three different visual fields. The mean value was calculated for statistical analysis.

Transmission electron microscopy

At the same time of section sampling for histological examination on day 3, week 1 (prior to the operation in Group B), and week 2, local soft tissues at the fracture site and bone specimens 2 mm from the fracture ends were sampled from two randomly selected dogs to observe cell growth under transmission electron microscopy. The samples were immediately placed in a 2.5% glutaraldehyde fixation solution at a temperature of 4°C for >2 hours. Gradient ethanol was used for dehydration, and epoxy resin (Epon 812; Structure Probe, Inc., West Chester, PA, USA) was used for embedding. The pellets were sliced into 1- to 2-μm sections. A LKB-V ultra-thin slicer (LKB Instruments, Stockholm, Sweden) was applied to create a slice thickness of 50 to 70 nm. After staining with uranium acetate and lead citrate, an H-7650 transmission electron microscope (Hitachi, Tokyo, Japan) was used for observation. Photographs of the soft tissues were obtained by the electron microscope at a magnification of 4000× on day 3 after fracture. The number of mesenchymal cells in 100 visual fields was counted for statistical analysis.

X-ray examination

Prior to killing of the dogs from the two groups at weeks 2, 4, and 8 following fracture, the affected limbs were examined by digital X-ray imaging to observe the callus status. A square grid with a side length of 1 mm was used to measure the number of grids with bone defection for the statistical analyses.

Statistical analysis

Continuous data conforming to a normal distribution are described as mean ± standard deviation, and SPSS 22.0 (IBM Corp., Armonk, NY, USA) was used for the statistical analyses. Student's t test was used to explore differences between groups. P-values of <0.05 were considered statistically significant.

Results

Gross observation of the fracture sites

Table 1 describes the gross observation findings of the fracture site at various time

Table 1. Observation of soft tissue at the fracture plane by histological examination and electron microscopy

	Histology		Electron microscopy	
Group (time point)	Group A (early surgery)	Group B (delayed surgery)	Group A (early surgery)	Group B (delayed surgery)
Day 3	Severe muscle cell swelling; large amount of neutrophils	Mild muscle cell swelling; small amount of neutrophils	Fibroblasts; numerous necrotic inflammatory cells; broken and scattered collagen fibrils	Cell proliferation; visible juvenile cells, mesenchymal cells, and macrophages
Day 7 (Group B, preoperatively)	Rare fibroblasts; necrotic tissues; calcium deposition	Numerous fibroblasts and osteoblasts; osteoid callus necrosis and pyknosis	Fibroblasts and occasionally visible newly formed capillaries	Mesenchymal cell proliferation; commonly visible newly formed capillaries
Week 2 (Group B, postoperative week 1)	Numerous scars composed of mature fibers; muscle atrophy	Granulation-covered fracture ends; fibroblasts and collagenous fibers within granulation; fibrous osteogenesis	Abundant capillaries	Numerous collagen granules and capillaries
Week 4 (Group B, postoperative week 3)	Interface of scar and sequestrum	Fibrous osteogenesis	–	–
Week 8 (Group B, postoperative week 7)	Interface of scar and sequestrum	Fibrous osteogenesis	–	–

points (Figures 2–10). The animals in Group A showed severe edema and a large amount of exudates from the wound 3 days after fracture. A 2- to 4-mL necrotic cavity filled with effusion around the fracture ends was observed after 1 week. At 2 weeks, the effusion had gradually absorbed. At 4 weeks, no visible callus was present, the fracture ends had begun to absorb, and the fracture gap was filled with scar tissue. The steel plates were loose in two dogs, while bone growth was almost stagnant. At 8 weeks, visible callus was still absent and the fracture ends were continuing to absorb, but the bone growth was still in a stagnant state, which led to atrophic nonunion.

The animals in Group B showed moderate edema 3 days after fracture. After 1 week (on the day of the operation), the edema was completely diminished and the fracture ends were coated by granulation tissue. At 2 weeks (postoperative week 1), callus was visible at the contralateral and lateral steel plates. At 4 weeks (postoperative week 3), bridge grafting of bony callus was present. At 8 weeks (postoperative week 7), the callus was healed. One steel

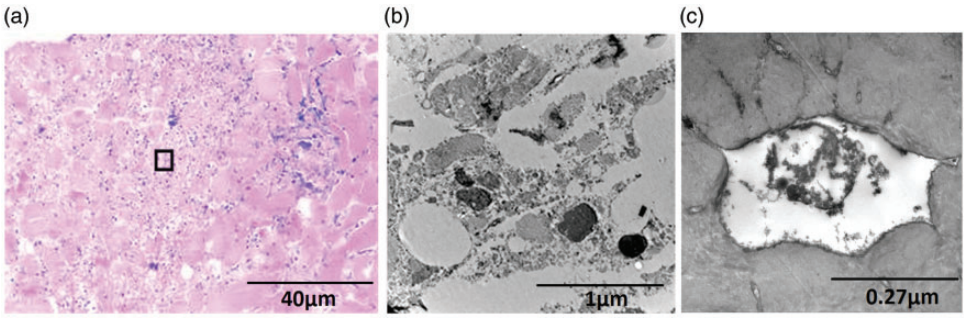

Figure 2. Soft tissues in the fracture plane of the early operation group 3 days following fracture. (a) Severe swelling of muscle cells and numerous degenerative neutrophils were observed (hematoxylin and eosin staining; magnification, ×100). (b) Electron microscopy indicated a large amount of necrotic inflammatory cells as well as ruptured and scattered collagen fibrils between muscle cells (magnification, ×4000). (c) Electron microscopy showed bone osteoblast necrosis (magnification, ×15,000).

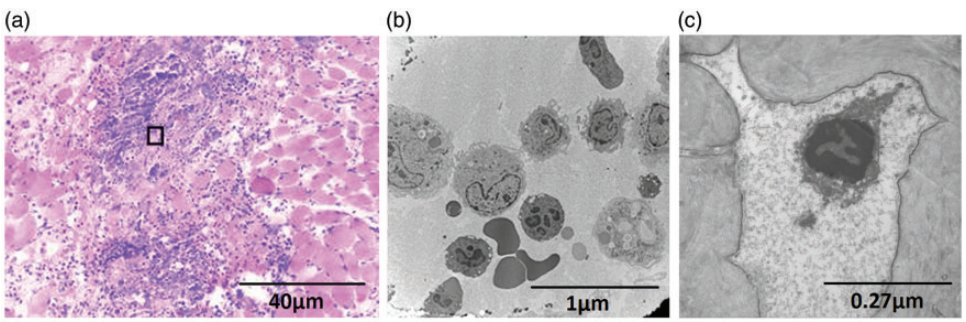

Figure 3. Soft tissues in the fracture plane of the delayed operation group 3 days following fracture. (a) Mild swelling of muscle cells and a small number of degenerative leukocytes were observed (hematoxylin and eosin staining; magnification, ×100). (b) Electron microscopy showed a variety of regenerated cells between muscle cells (magnification, ×4000). (c) Electron microscopy showed bone osteoblast apoptosis (magnification, ×15,000).

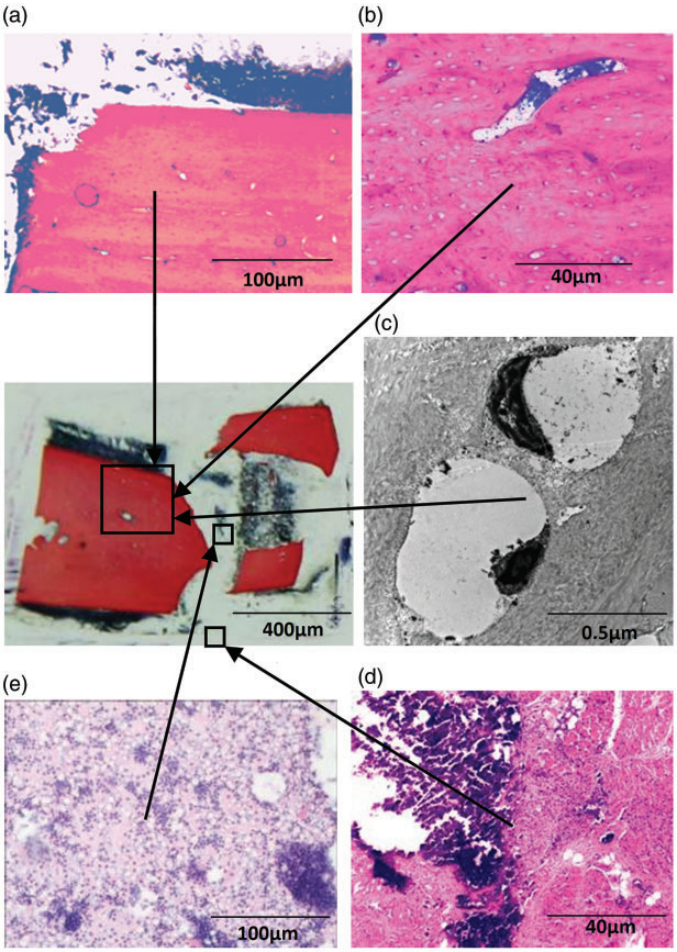

Figure 4. Seven days following fracture in the early operation group. (a) No callus surrounded the fracture ends (magnification, ×40). (b) Void bone lacunas (magnification, ×100). (c) Plastic section of the fracture segment (van Gieson's staining; magnification, ×10). (d) Electron microscopy showed karyopyknosis in void bone lacunas and endolysis (magnification, ×8000). (e) Deposition of calcium salts in adjacent necrotic muscle tissue and no repair of fibroblasts (HE staining; magnification, ×40). (f) Effusion around the fracture ends contained a large number of degenerative leukocytes and phagocytes (HE staining; magnification, ×100). HE, hematoxylin and eosin.

plate was loose, which led to a broken callus.

Histological examination

The observation findings of the soft tissues in the two groups of dogs at various time points are presented in Table 1 and Figures 2 to 11, and the observation findings of the bone tissues in the two groups are presented in Table 2 and Figures 2 to 11. At 3 days following fracture, light microscopy of soft tissues from Group A indicated that the muscle cells were swollen and a large number of neutrophils had infiltrated the region (the number was 20-fold higher than the number in Group B at 3 days after fracture, $P < 0.01$)

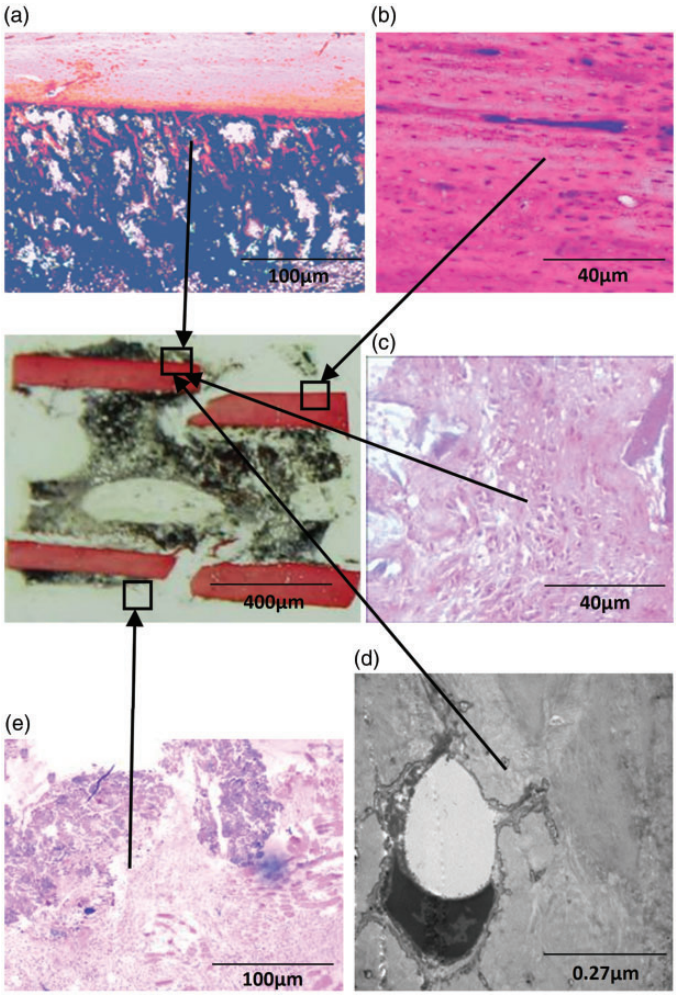

Figure 5. Seven days following fracture (on the day of the operation) in the delayed operation group. (a) Weak external callus had begun grow outside the cortex of the fracture ends (magnification, ×40). (b) All lacunas were void (magnification, ×100). (c) Fibroblasts adjacent to the sequestrum had begun to transform into bony callus (HE staining; magnification, ×100). (e) Normal muscle in adjacent tissues, pyknosis of necrotic tissues, repair of numerous fibroblasts, and no exudates from the fracture ends were observed (HE staining; magnification, ×40). (d) Electron microscopy showed bone cell apoptosis in void bone lacunas (magnification, ×15,000). HE, hematoxylin and eosin.

(Figure 2(a)). Electron microscopy demonstrated that a large number of necrotic inflammatory cells and scattered collagen fibers were present in the soft tissues (Figure 2(b)), and analysis of bone tissues revealed the presence of bone osteonecrosis. Electron microscopy analysis of tissues from Group B revealed a large number of proliferating mesenchymal cells in the soft tissues (for every 100 visual fields, 286 mesenchymal cells were found at a magnification of 4000×, and the difference was significantly different from that in Group A; $P < 0.01$) (Figure 3(a)). Additionally,

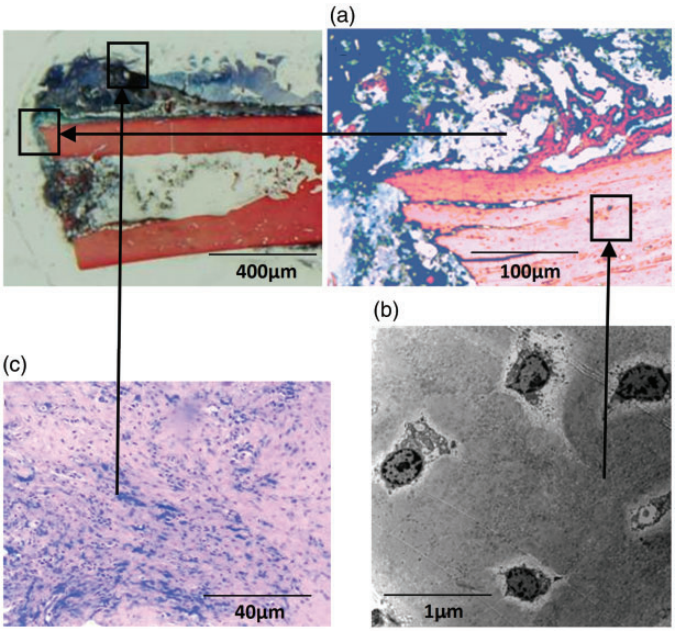

Figure 6. Two weeks following fracture in the early operation group. (a) Plastic section of the fracture segment (van Gieson's staining; magnification, ×10). (b) Weak callus growth outside the bone cortex and no callus in the fracture gap was observed (magnification, ×40). (c) Mature fiber cells in the adjacent tissues had progressed to form scar tissue (hematoxylin and eosin staining; magnification, ×100). (d) Electron microscopy showed a variety of bone cells in bone lacunas (magnification, ×4000).

bone cell apoptosis was present in the bone tissues. Seven days following fracture, light microscopy analysis of tissues from Group A revealed necrotic tissue, calcium salt deposition, and no fibroblasts in the soft tissues, and electron microscopy demonstrated occasionally visible newly formed capillaries in the soft tissues and bone cell regeneration in the bone tissues (Figure 4). Light microscopy analysis of tissues from Group B at 7 days following fracture showed a large number of fibroblasts, osteoid callus, and necrosis pyknosis in the soft tissues, and electron microscopy revealed marked mesenchymal cell proliferation and capillary hyperplasia in the soft tissues and bone cell apoptosis in the bone tissues (Figure 5). At 14 days following fracture, light microscopy analysis of tissues from Group A indicated that the mature fibers were scarring in the soft tissue and that the fracture space and bone did not exhibit callus growth (Figure 6). Electron microscopy showed a large number of capillaries in the soft tissue and bone marrow regeneration in the bone tissues (Figure 6). In Group B, light microscopy demonstrated that collagen granules covered the bone ends, a large number of new calluses had formed on the contralateral side of the bone, and a fibrous osteogenesis interface was present in the callus (Figure 7). The cutting cones and closing cones were reconstructed. Electron microscopy revealed a large number of collagen fibers, granulation, and capillary hyperplasia in the soft tissue. Bone cell apoptosis was present in the bone tissues (Figure 7). Four weeks after fracture, the fractures in Group A were scarring and the bone was slightly

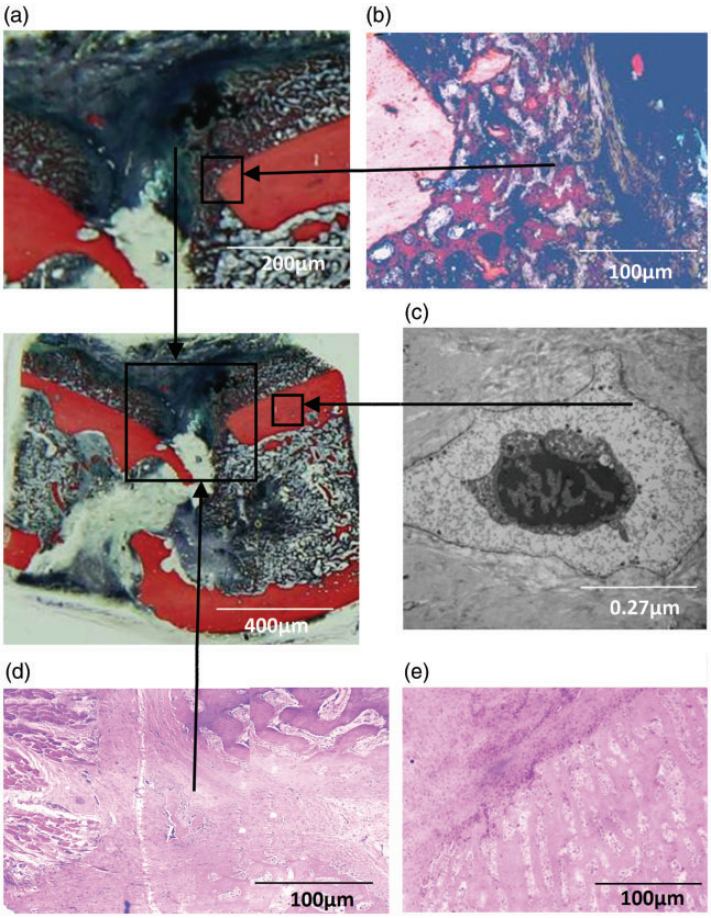

Figure 7. Two weeks following fracture (postoperative week 1) in the delayed operation group. (a) The callus at each end was about to converge (magnification, ×20). (b) Callus at one end (magnification, ×40). (c) Plastic section of the fracture segment showed a large amount of callus that had grown from the fracture ends in the intramedullary, extramedullary, and fracture gap directions (van Gieson's staining; magnification, ×10). (d) Electron microscopy showed bone cell apoptosis (magnification, ×15,000). (e) The callus had converged and generated interface with the external layer of muscle (HE staining; magnification, ×40). (f) Fiber osteogenesis interface under the granulation (HE staining; magnification, ×40). HE, hematoxylin and eosin.

atrophic (Figure 8). Group B (3 weeks postoperatively) showed bone callus bridging (Figure 9(a)) and new callus containing a rich and energetic cutting cone (osteoclast population) and closing cone (osteoblast population) extending in different directions[14]; the cutting cone was destroying the sequestrum, trailing the closing cone directly into the bone (Figure 9(b) and (c)). At 8 weeks after fracture, the original bone in Group A was thinner and had been replaced by new bone, which was blocked by scar tissue and unable to extend to the contralateral and surrounding regions, and atrophic nonunion had formed (Figure 10). Group B (7 weeks postoperatively) showed callus bridging at the bone endplates (Figure 11).

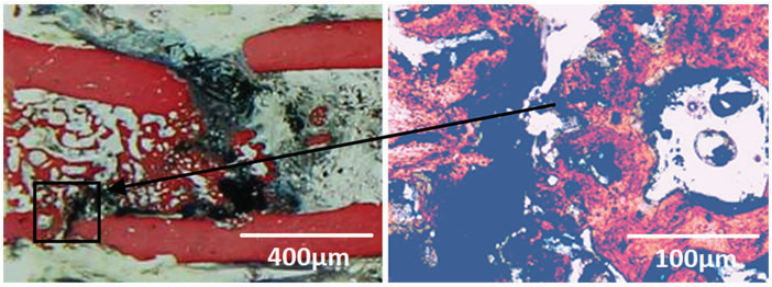

Figure 8. Four weeks following fracture/surgery in the early operation group. (a) Plastic section of the fracture segment showed a short and oblique scar barrier from the fracture gap and mild atrophy at the fracture ends (van Gieson's staining; magnification, ×10). (b) Magnified window displaying the nonunion gap (magnification, ×40).

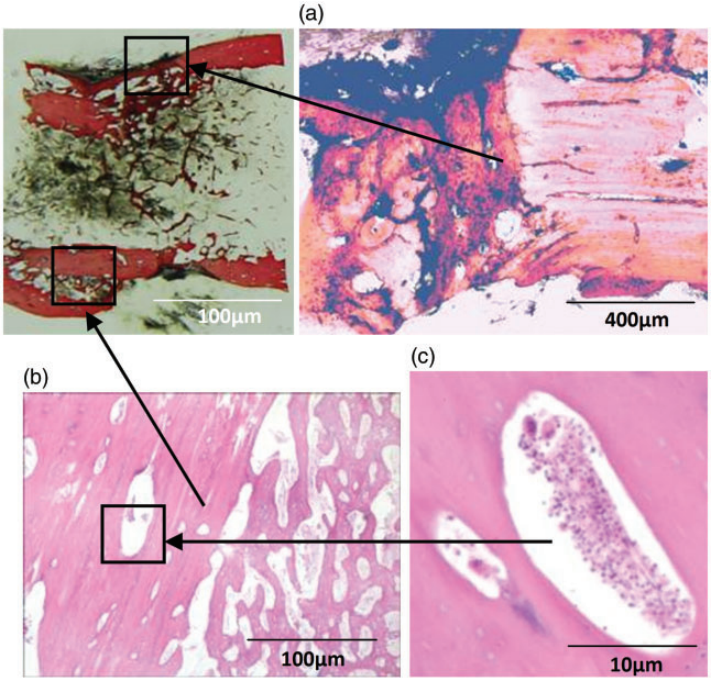

Figure 9. Four weeks following fracture in the delayed operation group (postoperative week 3). (a) Callus bridge (magnification, ×40). (b) Plastic section of the fracture segment indicated bridge grafting of bony callus (van Gieson's staining; magnification, ×10). (c) The newly generated callus contained abundant vital cutting cones (osteoclast cluster) and closing cones (osteoblast cluster) that pointed in different directions. The cutting cones were damaging the sequestrum and trailing the closing cones, which were directly osteogenic (hematoxylin and eosin staining; magnification, ×40). (d) Cutting cone and closing cone (magnification, ×400).

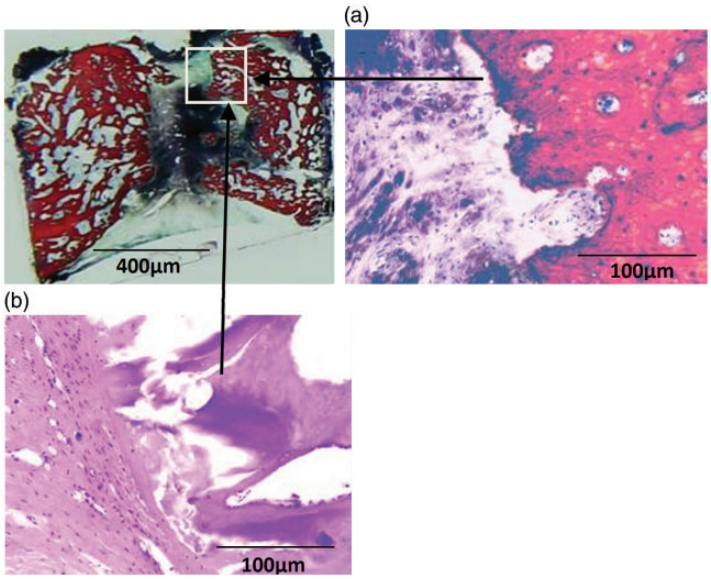

Figure 10. Eight weeks following fracture/surgery in the early operation group. (a) One end of the fracture (magnification, ×40). (b) Plastic section of the fracture segment indicated that the original sequestrum had absorbed and thinned and had been replaced by new bone, which was blocked by scarring and was unable to grow toward the contralateral side and to the surrounding area, thereby generating atrophic nonunion (van Gieson's staining; magnification, ×10). (c) Interface of scar and sequestrum (hematoxylin and eosin staining; magnification, ×40).

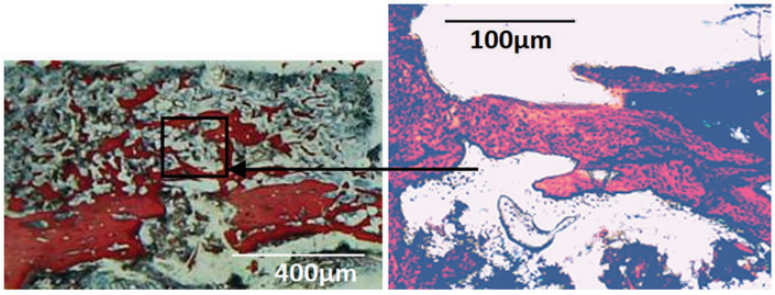

Figure 11. Eight weeks after fracture in the delayed operation group (postoperative week 7). (a) Plastic section of the fracture segment showed bridge grafting of bony callus in the lamellar layer (van Gieson's staining; magnification, ×10). (b) Lamellar bone callus (magnification, ×40).

X-ray examinations

Figure 12 shows representative X-ray images. Two weeks following fracture, no visible callus was present on X-ray images in either group. Four weeks following fracture in Group A, no callus was observed, the fracture ends had begun to shrink, and the fracture gap was slightly widened; in Group B, no bony callus was observed and the fracture gap was not widened. Eight weeks following fracture in Group A, atrophy of the fracture ends was visible,

Table 2. Observation of bone tissue at the fracture site by histological examination and electron microscopy

	Light microscopy		Electron microscopy	
Group (time point)	Group A (early surgery)	Group B (delayed surgery)	Group A (early surgery)	Group B (delayed surgery)
Day 3	Numerous void lacunas	Numerous void lacunas	Void bone lacunas; bone cell rupture	Void bone lacunas; bone cell apoptosis
Day 7 (Group B, preoperatively)	Void of all lacunas	Void of all lacunas; osteoid callus of osteoblasts on bone surface	Numerous fibroblasts	Void bone lacunas; bone cell apoptosis
Week 2 (Group B, postoperative week 1)	Slender callus in thin layer; scar in fracture gap	Sequestrum damaged by cutting cone; closing cone osteogenesis	Bone cells; osteoblasts	Bone cell apoptosis
Week 4 (Group B, postoperative week 3)	Fracture gap widened by 3 mm; scar blockage	Bridge grafting of bony callus	–	–
Week 8 (Group B, postoperative week 7)	Fracture gap blocked by scar	Lamellar bone callus	–	–

the fracture gap was widened, and atrophic nonunion was present. The area of bone absorption covered 48 grids, which was significantly different from Group B ($P < 0.01$). In Group B, no further absorption was present at the fracture ends, and callus surrounded the fracture ends and completely filled the fracture gap, thereby generating callus healing that filled in the fracture gap, the drill hole defects, the depression caused by angulation, and the small steps caused by dislocation.

Discussion

Although the fractures caused by high-energy injury and surgical damage were comparable between the two groups in the present study, the healing approach was completely different. In Group A, no callus was present at 1, 2, 4, and 8 weeks following fracture, resulting in atrophic nonunion. In Group B, a visible weak external callus was present 1 week after the fracture, and a good external callus growth mechanism was triggered at 2, 4, and 8 weeks, leading to callus healing. These findings suggest that the first week is critical for fracture healing. Absence of callus in the early stage means absence of callus growth throughout the entire healing process, while the presence of callus in the early stage leads to vigorous callus growth thereafter.

Perren[18] suggested that fracture end absorption is caused by unstable fixation. In the present study, the mechanical stability and destruction of blood flow in the two groups were identical; thus, the fracture end absorption in Group A may have been caused by the instability induced by lack of growth and the environment of severe inflammation at the fracture ends, which led to osteoclastic activity with absence of osteoblastic activity. Meanwhile, in Group B, the environment of mild inflammation successfully initiated callus growth, and

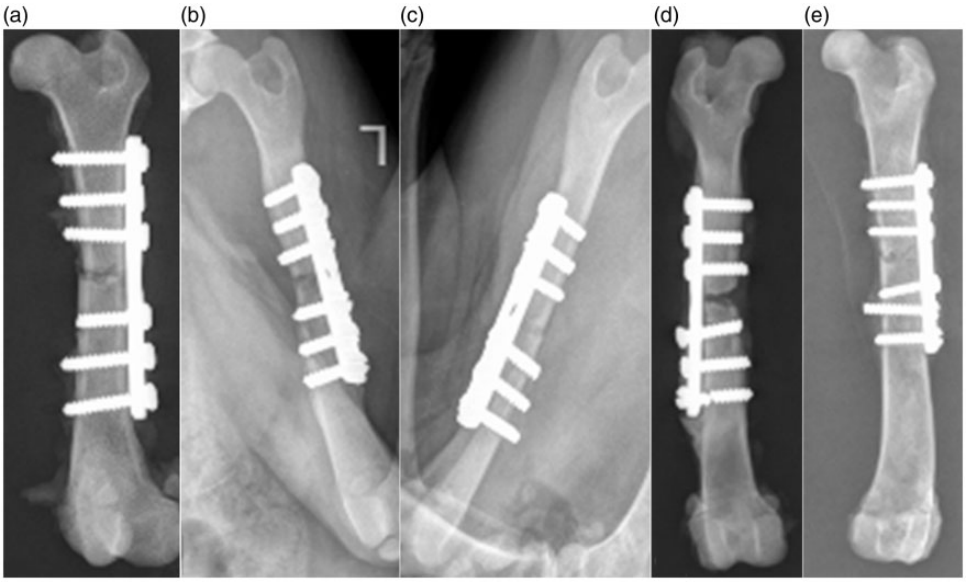

Figure 12. Postoperative X-ray films. (a) Postoperative week 2 in the early operation group. (b) Postoperative week 4 in the early operation group; a clear and slightly widened bone fracture slit was visible. (c) Postoperative week 4 in the delayed operation group; a non-widened, blurred bone fracture slit was observed. (d) Postoperative week 8 in the early operation group; the bone fracture gap was widened and separated, the fracture ends were withered, and nonunion was present. (e) Postoperative week 8 in the delayed operation group; callus surrounded the fracture ends and filled in the fracture gap, which had generated callus healing that completely filled in the fracture gap, the defects generated by the drilling holes, the depression caused by angulation, and the small steps caused by dislocation.

the stability provided by the steel plate fixation was preserved.

For ordinary low-energy fractures, the formation of a hematoma in the fracture gap induces the formation of or transition to osteoblasts, leading to bone growth.[19] In these fractures, the timing of the surgical intervention is unlikely to exert a significant effect on fracture healing.[15,16,20] In the present study, however, our model of high-energy fracture with significant soft tissue trauma revealed a large segment of void bone lacuna at the fracture site instead of cartilage islands far from the bone, indicating that the fracture end would become necrotic. This suggests that the early activity of fracture healing may be focused on the surrounding soft tissues. In fact, an obvious difference in callus growth was present between the early and delayed operation groups.

In the early operation group, the fracture ends were absorbed, the fracture gap was widened and blocked by scar tissues, and the callus was unlikely to extend to the contralateral side. In the delayed operation group, a newly generated and longitudinally aligned callus band first appeared on the bone surface at one site on the contralateral or lateral side. This callus band quickly replaced the "original dead sequestrum," grew rapidly, and broke through the fracture gap at an early stage and bridged with the contralateral side, thereby generating callus healing resembling a primary union.

The traditional method of preparing animal models of fracture nonunion involves the creation of a bone defect with

a diameter equal to the bone graft or wrapping of the fracture ends.[20] In the present study, a fracture model was developed simply by stabbing the surrounding tissues with the fracture ends instead of generating a bone defect or wrapping the fracture end, and atrophic nonunion was successfully established. This indicates that excessive, severe soft tissue injury alone can damage the external callus growth mechanism and lead to atrophic nonunion,[21] but a delayed operation to repair the same degree of soft tissue injury appears to restore the external callus growth mechanism and result in exuberant callus growth. However, this may not provide a sufficient explanation for the huge difference in healing between fractures with the same degree of traumatic and surgical blood supply injury. It may be hypothesized that delayed surgery after fracture may lead to different inflammatory reaction processes in the early phase of fracture.[22–28] When an early operation is performed, the inflammatory reactions of the primary injury may overlap with those of the surgical injury, leading to an excessive inflammatory reaction. When delayed surgery is performed, however, the inflammatory reactions of the primary injury are separated from those of the surgical injury. Additional studies are required to comprehensively examine these processes.

In the early stage following fracture, the inflammatory reaction was benign, local muscle cell swelling was mild at 3 days after the fracture, histological examination revealed a small amount of neutrophil infiltration, and electron microscopy revealed proliferation of a variety of cells between muscle cells. Seven days after fracture, fibroblasts adjacent to the sequestrum began to transform into a bony callus formed by osteoblasts, which represented the triggering of the first callus; this suggests that the operation in Group B was performed after this important biological step had occurred and after the inflammation process in response to the primary injury was completed.

Most traditional theories of fracture healing emphasize the independent effect of the blood supply. A study by Brownlow et al.[12] demonstrated that recovery of the blood supply at the fracture site within 1 week after fracture was the most important factor for healing. Although the present study also revealed proliferation of newly formed capillaries 7 days after fracture in the delayed operation group, proliferation of a variety of cells in the surrounding tissues was already present 3 days after fracture. This suggests that the early induction activity of various primitive cells was already underway prior to the effective formation of new capillaries and indicates that the early induction environment may not rely on an effective newly formed blood supply; instead, it may be more likely to depend on the residual blood supply and interstitial fluid. Because the residual blood supply was similar between the two groups, benign inflammation may be the key factor. This renewable environment may be a benign interstitial fluid environment referred to as fracture exudate by Hulth[20] and is generated by the early benign inflammatory response induced by the undisturbed primary fracture hematoma. However, because the primary soft tissue injury is mild in ordinary low-energy fractures, the sum of its effect and that of the operative injury may still lead to benign inflammation, which results in an insignificant effect of an early or delayed operation on healing.

Novel technologies have been designed for the application of minimally invasive techniques to increase the healing rate of fractures and prevent nonunion by stimulating callus growth. Minimally invasive techniques reduce the severity of operative injury and thus promote the healing of low-energy fractures. However, these technologies are unable to diminish or alleviate pre-hospital injuries such as primary injury

or transport injury in patients with high-energy fractures. In addition, delayed surgery fails to diminish pre-hospital injury. However, preoperative closed reduction and effective reduction may initiate the healing process of inflammatory response (or immune response) caused by pre-hospital injury, and then the surgical injury was performed.[22,29,30] The present study revealed that repair of soft tissues after stabilization of the reduction helped to protect the immune response of the original hematoma.[29] Thus, the callus response during the first postoperative week in the delayed operation group was the first callus response initiated by the primary injury. This indicates that the injury induced by delayed open reduction is unlikely to affect the callus that had already been initiated and that the surgery induces a secondary wound healing response,[9] thereby maximizing the callus growth capability of the fracture and resulting in exuberant callus growth. In addition, delayed surgery is applicable to patients who are unable to undergo minimally invasive surgery.

In the present study, we induced open mini-hole fractures to establish a midpoint transverse fracture of the femoral shaft (i.e., a Kirschner wire was used to drill a hole in the femur through the skin, leaving a tiny sterile pinhole in the skin). Gustilo[31] reported that the infection rate of type I open fracture is 0%, and the treatment principles are identical to those for type I closed fracture. Therefore, the models in the present study effectively mimicked closed high-energy fractures. Actually, high-energy fractures are generally open fractures, while open fractures are also generally high-energy fractures. The poor outcomes of high-energy fractures have generally been attributed to contamination of the open wound, comminution of the fracture, and destruction of the blood supply by surgeons. However, the substantial destruction of the biological environment induced by extensive muscle contusion are commonly ignored because muscle contusion cannot be easily detected by routine examination methods (such as X-ray), especially for type I open or closed high-energy fractures. Tscherne and Oestern[32] classified the degrees of closed soft tissue injuries combined with fractures; however, they did not mention internal muscle injuries that had no signs of external soft tissue injuries. The destructive effects of simple muscle contusion on the biological environments in fractures have not been sufficiently investigated; thus, no practical and effective treatment strategies are available in clinical practice. We therefore designed the present experimental models of atrophic nonunion induced by simple muscle contusion, which reflects the effects of simple muscle contusion on the destructive processes that affect the biological environments of fracture. The findings could provide new ideas for the treatment of atrophic nonunion.

Conclusion

Extensive contusion of the muscles adjacent to the fracture is an important factor in destruction of the biological environment and leads to poor fracture healing. Immediate surgery can aggravate the inflammatory response, thus damaging the biological environment, preventing the formation of external callus, and leading to atrophic nonunion. Delayed surgery following effective closed reduction and immobilization can ameliorate the inflammatory response, protect the biological environment, stimulate active callus growth, and thus result in callus healing under fixation. The differences in healing after immediate versus delayed surgery are caused by the different early inflammatory responses induced by the differences in surgical timing, which lead to differences in callus growth in cases of high-energy fractures.

Declaration of conflicting interest

The authors declare that there is no conflict of interest.

Funding

The present study was supported by Science and Technology Plan Projects of Yulin City, Shanxi Province, China (grant no. 2014jh-38) and Science and Technology Project of Shaanxi Science and Technology Department (No. 2016SF-291).

ORCID iD

Zhijun Pan https://orcid.org/0000-0001-8856-422X

References

1. Bhadra AK, Roberts CS and Giannoudis PV. Nonunion of fibula: a systematic review. *Int Orthop* 2012; 36: 1757–1765.
2. Collinge C, Kuper M, Larson K, et al. Minimally invasive plating of high-energy metaphyseal distal tibia fractures. *J Orthop Trauma* 2007; 21: 355–361.
3. Austin RT. Fractures of the tibial shaft: is medical audit possible? *Injury* 1977; 9: 93–101.
4. Gonzalez del Pino J, Bartolome del Valle E, Grana GL, et al. Free vascularized fibular grafts have a high union rate in atrophic nonunions. *Clin Orthop Relat Res* 2004; (419): 38–45.
5. Copuroglu C, Calori GM and Giannoudis PV. Fracture non-union: who is at risk? *Injury* 2013; 44: 1379–1182.
6. Rupp M, Biehl C, Budak M, et al. Diaphyseal long bone nonunions - types, aetiology, economics, and treatment recommendations. *Int Orthop* 2018; 42: 247–258.
7. Yu L and Fenglin Z. High-energy tibial plateau fractures: external fixation versus plate fixation. *Eur J Orthop Surg Traumatol* 2015; 25: 411–423.
8. Westgeest J, Weber D, Dulai SK, et al. Factors associated with development of nonunion or delayed healing after an open long bone fracture: a prospective cohort study of 736 subjects. *Orthop Trauma* 2016; 30: 149–155.
9. Frost HM. The biology of fracture healing. An overview for clinicians. Part I. *Clin Orthop Relat Res* 1989; (248): 283–293.
10. Reed AA, Joyner CJ, Brownlow HC, et al. Human atrophic fracture non-unions are not avascular. *J Orthop Res* 2002; 20: 593–599.
11. Reed AA, Joyner CJ, Isefuku S, et al. Vascularity in a new model of atrophic non-union. *J Bone Joint Surg Br* 2003; 85: 604–610.
12. Brownlow HC, Reed A and Simpson AH. The vascularity of atrophic non-unions. *Injury* 2002; 33: 145–150.
13. Gomez-Benito MJ, Garcia-Aznar JM, Kuiper JH, et al. Influence of fracture gap size on the pattern of long bone healing: a computational study. *J Theor Biol* 2005; 235: 105–119.
14. Wullschleger ME, Steck R and Matthys R. A new model to study healing of a complex femur fracture with concurrent soft tissue injury in sheep. *Open J Orthop* 2013; 3: 32701.
15. Einhorn TA. The science of fracture healing. *J Orthop Trauma* 2005; 19: S4–S6.
16. Marsell R and Einhorn TA. The biology of fracture healing. *Injury* 2011; 42: 551–555.
17. Phillips AM. Overview of the fracture healing cascade. *Injury* 2005; 36: S5–S7.
18. Perren SM. Physical and biological aspects of fracture healing with special reference to internal fixation. *Clin Orthop Relat Res* 1979; 68: 175.
19. Seenappa HK, Shukla MK and Narasimhaiah M. Management of complex long bone nonunions using limb reconstruction system. *Indian J Orthop* 2013; 47: 602–607.
20. Hulth A. Current concepts of fracture healing. *Clin Orthop Relat Res* 1989: 265–284.
21. Hildebrand F, van Griensven M, Huber-Lang M, et al. Is there an impact of concomitant injuries and timing of fixation of major fractures on fracture healing? A focused review of clinical and experimental evidence. *J Orthop Trauma* 2016; 30: 104–112.
22. Schmidt-Bleek K, Schell H, Schulz N, et al. Inflammatory phase of bone healing initiates the regenerative healing cascade. *Cell Tissue Res* 2012; 347: 567–573.

23. Schmidt-Bleek K, Schell H, Lienau J, et al. Initial immune reaction and angiogenesis in bone healing. *J Tissue Eng Regen Med* 2014; 8: 120–130.
24. Bastian O, Pillay J, Alblas J, et al. Systemic inflammation and fracture healing. *J Leukoc Biol* 2011; 89: 669–673.
25. Loi F, Córdova LA, Pajarinen J, et al. Inflammation, fracture and bone repair. *Bone* 2016; 86: 119–130.
26. Chan JK, Glass GE, Ersek A, et al. Low-dose TNF Augments fracture healing in normal and osteoporotic bone by up-regulating the innate immune response. *EMBO Mol Med* 2015; 7: 547–561.
27. El-Jawhari JJ, Jones E and Giannoudis PV. The roles of immune cells in bone healing; what we know, do not know and future perspectives. *Injury* 2016; 47: 2399–2406.
28. Kolaczkowska E and Kubes P. Neutrophil recruitment and function in health and inflammation. *Nat Rev Immunol* 2013; 13: 159–175.
29. Kolar P, Schmidt-Bleek K, Schell H, et al. The early fracture hematoma and its potential role in fracture healing. *Tissue Eng Part B Rev* 2010; 16: 427–434.
30. Schell H, Lienau J, Epari DR, et al. Osteoclastic activity begins early and increases over the course of bone healing. *Bone* 2006; 38: 547–554.
31. Gustilo RB. Problems in the management of type III (severe) open fractures. A new classification of type III open fractures. *J Trauma* 1984; 24: 742–746.
32. Tscherne H and Oestern HJ. [A new classification of soft-tissue damage in open and closed fractures (author's transl)]. *Unfallheilkunde* 1982; 85: 111–115.